

A newly developed technique for enhanced cell growth in 3D scaffolds: Investigation of cell seeding and proliferation under static and dynamic conditions

Konstantinos Theodoridis¹, Elena Aggelidou¹, Maria Eleni Manthou¹, Kleoniki Keklikoglou², Antonios Tsimponis¹, Efterpi Demiri¹, Athina Bakopoulou¹, Athanasios Michailidis¹, and Aristeidis Kritis¹

¹Aristotle University of Thessaloniki

² Hellenic Centre for Marine Research

May 5, 2020

Abstract

Cell adhesion on 3D-scaffolds is a challenging task to succeed high cell densities and even cell distribution. We aimed to design a static 3D-cell Culture Device which limits cell loss, facilitates circulation of fluids and can be used with any scaffold. 3D printing technology was used for both scaffold and device fabrication. Apart from testing the device, the purpose of this study was to assess and compare static and dynamic methods and their effects on parameters such as cell seeding efficiency, cell distribution and cell proliferation in different culture conditions. Human adipose tissue was harvested and cultured in 3D-printed polycaprolactone scaffolds. Half the scaffolds were dry and the rest of them were prewetted. Micro-CT scans were performed and projection images were reconstructed into cross section images. We created 3D images to visualize cell distribution and orientation inside the scaffolds. The group of prewetted scaffolds was the most favorable to cell attachment. The 3D-cell Culture Device (3D-CD) enhanced cell seeding efficiency in static culture, with almost no cell loss. We suggest that the most favorable outcome can be produced with static seeding in the device for 24 hours, followed by proliferation either in the same device or with dynamic culture.

Introduction

Regenerative medicine, a multidisciplinary field, aims to apply various biological and engineering principles to regenerate tissues that will be used to overcome the limited availability of organ and tissue transplants and/or to replace damaged or lost tissues in human clinical applications (Langer & Vacanti, 1993; Lefterink et al., 2016). For this purpose, a cell isolation method is used to extract patient's own cells (autologous cells), usually from a small biopsy, and then the cells are seeded on an engineered 3D matrix (scaffold). The scaffolds, used as a cell carrier, have a predefined structure and are usually made from natural and/or synthetic biomaterials (Dawson et al., 2008; Nair & Laurencin, 2007).

Cell seeding is the first critical step for a successful 3D cell culture and therefore for tissue formation (G. Vunjak-Novakovic et al., 1998a). The optimal scaffold should support the tissue defect site in terms of mechanical and physicochemical properties but should also provide the appropriate micro-environment for cell growth and differentiation in vitro (Theodoridis et al., 2019). This micro-environment depends on the porosity, the pore sizes and their interconnected network (Fahimipour et al., 2019). Furthermore, the scaffold's pore network must be permeable to oxygen and nutrient transport for cell proliferation and differentiation capacity of MSCs (Lavrentieva et al., 2010; Merceron et al., 2010; Sheehy et al., 2012). It is clear that cultivation into optimal oxygen concentration is another important factor that affects cell expansion and differentiation.

Cell adhesion on the engineered grafts is a very challenging task. High cell densities and even cell distribution are very important, especially when a small biopsy or cells with low-proliferative capacity, such as chondrocytes, are used (Weinand et al., 2009). This is the reason why so much effort is put to improve cell seeding efficiency and distribution of cells. Various modifications on protocols have been suggested but the most well-established cell seeding methods can be categorized in two major techniques: the static cell seeding and the dynamic cell seeding. Due to its relative simplicity, the most common method is static cell seeding, where cells within a minimum volume of nutrients are suspended either on one surface (Choong et al., 2006; Hofmann et al., 2006; Rodina et al., 2016) or on both surfaces of the standing scaffold construct (Theodoridis et al., 2019). It has also been described that the aliquot of cell suspension may be pipetted up and down, for equal distribution inside the scaffold (Correia et al., 2012). Although static cell seeding method is generally recognized as an effective method, many studies indicate low cell seeding efficiencies (Fahimipour et al., 2019; Kim et al., 1998; Luo et al., 2013).

On the other hand, dynamic cell seeding has been reported to be a surplus on seeding efficiency and cell distribution. The most commonly used dynamic seeding technique has been established by Vunjak-Novakovic G. et al. and Freed L.E. et al. (Freed et al., 1998; G. Vunjak-Novakovic et al., 1998b). Cells are suspended within spinner flasks. The scaffolds are usually stationary but a magnetic stirrer creates a turbulent flow and suspended cells attach on the scaffolds by convection (Gordana Vunjak-Novakovic et al., 1996). Other techniques of dynamic cell seeding include perfusion bioreactors, oscillating techniques (Alvarez-Barreto & Sikavitsas, 2007; Weinand et al., 2009), or the use of custom-made devices, such as the U-cap bioreactor system described by Wendt et al. (Wendt et al., 2003).

In this study we used scaffolds made of polycaprolactone (PCL), manufactured according to own previous results suggesting the most favorable architecture to support cell attachment and proliferation. One of the drawbacks we detected in previous work is the attachment of cells on the surface of the well plate under the scaffold. Moreover, the dynamic culture, which is generally considered more favorable for the cells, has a higher risk of contamination and many limitations, mainly due to its complexity (Wendt et al., 2003). Considering the restrains, we aimed to design a static 3D-cell Culture Device (3D-CD) which limits cell loss during culture, facilitates the circulation of fluids and nutrient supplies within it and can easily be used with almost any kind of scaffold's shape. Cell adhesion on engineered autologous grafts is a very challenging task for cell growth and differentiation *in vitro*. The same 3D printing technology used in previous works for scaffold fabrication was also recruited for the construction of our static 3D-cell Culture Device (3D-CD). This device was designed to hold the scaffolds on air, so that all their surfaces are free and we tested whether the requirements we set were fulfilled.

Apart from testing this new device, the purpose of this study was to assess and compare static and dynamic methods and their effects on parameters such as cell seeding efficiency, cell distribution and cell proliferation in different culture conditions. We wish to add new information in this wide field of investigation and suggest the most favorable conditions for each and every studied parameter. The information will result in more efficient protocols for stem cell based regenerative applications.

2. Materials and Methods

2.1 Prototype 3D-cell Culture Device fabrication

We created a device that can hold scaffolds on air. Our device was based on standard dimensions of a 6-well plate format (Greiner Bio-One, GmbH) and the design draft is shown in figure 1A. The device was manufactured with a benchtop 3D-Printing machine PRUSA i3 (USA). Moreover, the Slice3r software was used for the entire geometry and the 'printing infill' was set to solid. The material for this device was polylactic acid (PLA, 3D4MAKERS, Netherlands) with a density of about 1.25 kg/cm³. After fabrication, the device was sterilized by immersing it in ethanol for 20 minutes and thereafter exposed to UV irradiation for 30 minutes. Thirty devices were required for this experiment.

2.2 Scaffold fabrication

Scaffold fabrication was processed by Fused Deposition Modeling (FDM) method using a benchtop 3D-Printing machine PRUSA i3 (USA). Cylindrical scaffolds, 10mm in diameter and 3mm in height, were composed from 10 layers of material (300 μ m thickness each), interconnected with a 3D honeycomb structure pattern and infill density of 60%, thus resulting to rectangular and hexagonal pores, ranging from 150-700 μ m (average of [?] 425 μ m) on the final constructs. This layer pattern was chosen because in our previous work it was shown to enhance cell colonization and infiltration (Theodoridis et al., 2019). Slice3r software was used for creating this geometry pattern. Polycaprolactone (3D4MAKERS, Netherlands), with a molecular weight of 50 kDa and a density of 1,145g/cm³, was used as a 3D filament with diameter of 1.75mm. The printing temperature was set at 145°C and the extrusion speed at 60mm/s. After fabrication, a total number of 65 PCL scaffolds were immersed in a 4MNaOH bath, for approximately 20h at room temperature (RT), to increase their surface hydrophilicity and clean their fibers.

2.3 Isolation, expansion and characterization of Adipose Derived Mesenchymal Stem Cells (ADMSCs)

Human adipose tissue (~ 70 ml) was harvested, from a lipoaspiration procedure, under Papageorgiou Hospital Review Board approved protocols, 263-7/12/2016, and patient informed consent. Human adipose derived stem cells (ADMSCs) were isolated, expanded and characterized in our cGMP facility. Cells were isolated and expanded in MSC medium, consisting of a-MEM, 15% FBS 2mM Glutamine, 0.1mM L-ascorbic acid phosphate, 100U/ml penicillin, 100mg/ml streptomycin. Isolated cells were characterized as Mesenchymal Stem Cells by a Guava® easyCyte 8HT flow cytometer (Merck-Millipore, Darmstadt, Germany). Cells expressed CD90 and CD73 (positive markers), whereas CD45 was used as a negative marker. Unstained cells were used as a control to set the gates and analysis as described in our previous work

2.4 Scaffold groups & seeding of ADMSCs

2.4.1. Scaffolds wet and dry

Two different groups were separated after hydrophilization. Half of the scaffolds were air dried in the laminar flow hood for 24hours (dry scaffolds), and the rest of them were further incubated with MSC medium for 24h in the incubator (wet scaffolds). We used four seeding techniques on dry scaffolds: 1) cell seeding only on one surface, designated as “SD1S” (Fig.2.I.A), 2) cell seeding on both surfaces, designated as “SD2S” (Fig.2.I.B), 3) one side cell seeding with the scaffold placed on our static 3D-cell Culture Device (3D-CD), designated as “SD1S-on Air” (Fig. 2.I.C), 4) both sides seeding with the scaffold placed on our device, designated as “SD2S-on Air” (Fig. 2.I.D). The wet scaffolds were treated accordingly and were designated: “SW1S”, “SW2S”, “SW1S-on Air” and “SW2S-on Air”.

2.4.2. Static seeding

Both groups (wet and dry scaffolds) were transferred on 6-well plates. The two different seeding techniques were applied and equal number of cells (1.5x10⁵ cells) was seeded to all of the scaffolds. For the one-side seeding technique, 20 μ l of MSC medium and the appropriate amount of cells were suspended on the top side of the scaffolds (Fig. 2.I.A, C). Scaffolds were then incubated at 37°C, 5% CO₂ humidified atmosphere for 2h to allow cell attachment on the scaffolds. 1.5 mL of MSC medium was added inside the wells.

For the double-side seeding technique, the same number of cells was seeded in two steps. First, half of the cells (0.75x10⁵ cells in 10 μ l MSC medium) were suspended on the top side of the scaffolds and were incubated at 37°C, 5% CO₂ humidified atmosphere for 60min. The rest of the suspension was seeded on the bottom side of the scaffolds and the incubation continued for another 60min (Fig. 2.I.B, D). 1.5 mL of MSC medium was then added to the wells.

2.4.3 Dynamic seeding

For the dynamic seeding we used spinner flasks onto magnetic stirrers (DWK Life Sciences, WHEATON-Micro-Stir®). Briefly, the cap of each spinner flask was drilled with holes, in which we placed 24Gx90mm needles (Spinal Needle, Polymed Belgium). The needles were used to hold the scaffolds, designated “Dynamic-

Stirrers". Two extra holes were made on each cap to ensure gas circulation, as shown in figure 2. II. Culture medium, 70 mL, was added in each flask with the empty scaffolds and was left 24h inside the incubator. After 24 hours, 20mL of this medium was removed, was then mixed with an amount of 1.5×10^5 cells/scaffold and was finally resuspended inside the spinner flask with the scaffolds. In the meantime, the magnet within the flask was rotating on 50rpm, creating a turbulent flow.

2.5 Cell proliferation in static and dynamic culture, under Normoxia and Hypoxia

The scaffold with the best performance 24 hours after seeding, ie SW2S-on Air, and the wet scaffold on the dynamic stirrer, whose behavior we intended to investigate, were both chosen to proceed with cell expansion. Both techniques (static and dynamic) were evaluated for cell proliferation after 6 days, under two different culture conditions, in normoxia (20% O₂ and 5% CO₂) and in hypoxia (5% O₂ and 5% CO₂).

In static culture we changed the nutrients every two days. In dynamic culture we removed half of the medium on the 3rd day and replaced it with fresh one. The stirring settings remained the same for the 6-day culture period.

2.6 Confocal Microscopy (Live/Dead Assay)

ADMSC seeded scaffolds, were evaluated for cell viability and colonization after 24h and 6 days respectively. Viability/Cytotoxicity Assay Kit for Animal Live & Dead Cells was used (#3000, Biotium, CA, USA), according to the manufacturer's instructions. Samples were visualized by a confocal upright fluorescence microscope (Nikon D-Eclipse 80i C1). For live/dead staining, ADMSCs/scaffold constructs were double stained with calcein AM and ethidium homodimer, staining living and dead cells, respectively. After adding both dyes, the constructs remained at RT in the dark for 30min and before visualization they were washed with PBS. The constructs were captured as z-stack images using the EZ - C1 3.20 software.

2.7 Cell counting

For cell counting we used 3D Biotek's protocol to detach cells from the scaffolds. We removed cell culture media and rinsed the scaffolds two times with 1xPBS. We immersed scaffolds in Trypsin- EDTA (0.25 %) enzyme solution and placed the cell culture plate onto an agitating shaker inside the incubator for 20 minutes at 37°C. After cells were detached, we added a-MEM growth media at a volume equal to the original enzyme solution for neutralization. We then gently pipetted the cell suspension up and down ~5X's within the scaffold in order to flush out the remaining cells from the scaffold. Finally, we centrifuged down the cells for 3 min at 1,000rpm and resuspended them in 500ul PBS in order to count them via Guava® easyCyte 8 flow cytometer. Correlated measurements of side-scattered light (SSC) and forward-scattered light (FSC) were used for absolute cell counting. More specifically, a polygonal region was created on the FSC vs SSC plot and the data acquired were analyzed automatically by InCyte™ software. Each stat was derived from the polygon region that was set in order to separate cells from debris, as shown in figure 3.

2.8 Micro-Computed Tomography

2.8.1 Cell renderings and cell particles visualization

Micro-CT scans were performed at the Hellenic Centre for Marine Research (HCMR) using a Skyscan 1172 micro-tomograph (Bruker, Kontich, Belgium). This scanner uses a tungsten X-ray source which is equipped with an 11MP CCD camera (4000 x 2672 pixel). All specimens were scanned at a voltage of 59KV and 167µA without filter for a full rotation of 360° at the highest camera resolution. Projection images were reconstructed into cross section images using the SkyScan's NRecon software (NRecon, Bruker, Kontich, Belgium) which implements a modified Feldkamp's back-projection algorithm. All scans were loaded into the CTVox software (CTVox, Bruker, Kontich, Belgium) in order to graphically represent the proportion of the area occupied by the cells inside the scaffold, and 3D rendered images of the scanned specimens were created to visually represent the total orientation of the cells inside scaffolds (Fig. 6).

2.8.2 Image compilation and distribution analysis

We divided each studied scaffold in 3 zones, a top, middle and a bottom. Approximately 500 slices (scans) from each scaffold were taken with micro-CT, while the step/slice was set at a $6\mu\text{m}$ in Z direction. In total, 300 slices were analyzed and specifically 100 slices from each zone. These slices were analyzed for distribution and agglomeration of the cells at two time points, after adhesion at 24h, and after proliferation at the 6th day. The 2D slices of each data set were imported as an image sequence and then were stacked, using Image J. All of these images were converted in 8-bit images and a common threshold area was applied for all measurements, so that we can visualize only cells and cell clusters, avoiding the scaffold material. The “3D OC option” settings were adjusted to account only the surfaces of the sections after the thresholding procedure. Furthermore, the “3D Objects Counter” was set to a size filter appropriate for analyzing cells. Every dataset of each scaffold was then scanned using the 3D object counter, which combined the 2D surfaces in stack surfaces (Bolte & Cordelieres, 2006). All of the stacked surfaces were then merged to a composite 3D image, using the 3D projection tool with interpolation. Finally, we expressed the percentage of the total area of the scaffold occupied by the cell population. In addition, we used the “Interactive 3D Surface Plot” to better visualize the cell arrangement in 3D graphs, as a histogram (Fig. 7.A, B and Fig. 8.A, B).

2.9 Statistics

Results are presented as mean \pm SD for $n=3$ biological replicates. One-way ANOVA was used to analyze results of cells counting from flow cytometer in order to compare the cell adhesion of ADMSCs within the scaffolds under different seeding techniques. Multiple comparisons between groups were performed with Tukey’s post-hoc test, using Prism 6.0 Software (GraphPad, CA, USA). Differences between means were considered statistically significant when $*p\text{-values}<0.05$.

3. Results

3.1 Scaffold porosity

Scaffold’s porosity was measured by two methods, the gravimetric method and the Image J method, to calculate the porosity as described from other studies (Karageorgiou & Kaplan, 2005; Loh & Choong, 2013; Martinez-Ramos et al., 2012; Theodoridis et al., 2019). The material density was calculated using the bulk and the true density of the scaffold ($n=3$), according to the equations 1 and 2 below,

$$\rho_{\text{scaffold}} = \frac{\text{mass}}{\text{volume}} \quad (1)$$

$$\text{Total porosity, } P_t = 1 - \frac{\rho_{\text{scaffold}}}{\rho_{\text{material}}} \quad (2)$$

where ρ_{scaffold} = apparent density of the scaffold, and ρ_{material} = density of the material. The outcomes are presented in Table 1 as mean \pm SD for three independent measurements.

3.2 Evaluation of cell viability – Confocal Microscopy

The primary objective of the study was to determine the most advantageous methods for seeding efficiency of ADMSCs (cell adhesion) to a 3D scaffold. For this purpose, we used a 3D honeycomb pattern and tested eight different methods for static seeding and one method with dynamic seeding. We assessed cell viability after 24h and after 6 days, on the surfaces of the scaffolds and on cross sections. After 24h, cells were viable in all scaffolds (Fig. 4.A). It seems that the wet scaffolds in static culture carried more viable cells compared to the dry scaffolds. On the other hand, the wet scaffold in dynamic culture does not seem to have many viable cells, especially as seen in cross sections.

By the 6th day the majority of cells remained viable, with no significant dead cell batches, in all scaffolds. Cell viability in dynamic culture seems to be much higher compared to the static culture, both on the surface of the scaffolds and in cross sections (Fig. 4.B). Scaffolds cultured under normoxic conditions carried more cells compared to the respective scaffolds cultured in hypoxia (Fig. 4.B.I, III static and 4.B.V, VII dynamic).

3.3 Evaluation of absolute cell counting with Flow Cytometer

Scaffolds with the most favorable performance were the static, wet scaffolds, seeded on both or only one side. The wet scaffolds on air (SW1S-on Air and SW2S-on Air) exhibited the least, non significant cell loss, making

them the optimal scaffolds for static seeding. The SW1S and the SW2S performed very well too. The wet scaffold on the dynamic stirrer on the other hand, exhibited a significant cell loss and was the least favorable scaffold for cell adhesion 24 hours after seeding. The dry scaffolds also exhibited high cell loss 24 hours after seeding. Either dry scaffolds were seeded on one or on both sides, cell adhesion was poor when compared to the wet scaffolds.

The scaffold with the best performance 24 hours after seeding, ie SW2S-on Air, and the wet scaffold on the dynamic stirrer, whose behavior we intended to investigate, were both chosen to proceed with cell proliferation, under two different conditions, normoxia and hypoxia. As shown on the diagram (Fig. 5) at the 6th day all scaffolds exhibited an increase in their cell population. The scaffolds with the best performance were those of the dynamic stirrer. Even though their initial cell populations were much lower than the corresponding on SW2S-on Air scaffolds, six days of proliferation led to an impressively higher increase and finally to a significantly higher number of cells on the dynamic scaffolds (20fold increase for the dynamic stirrer scaffold and 2,6fold increase for the SW2S-on Air scaffold). Overall normoxia seemed to be favorable compared to hypoxia, nevertheless, not significantly.

3.4 Evaluation of cell distribution scanned with micro - Computed Tomography

24 hours after cell culture we evaluated cell distribution within the 3 representative zones of each scaffold (Fig. 7). We were obviously mostly interested to study cell distribution in the scaffolds with no significant cell loss, therefore we focused on SW1S, SW2S, SW1S-on Air, SW2S-on Air. Scaffolds seeded on both sides exhibited a better, more uniform distribution of cells within all zones. On the other hand, cells in scaffolds seeded on one side were mostly found on the upper and middle zones, therefore the distribution was more uneven. Surprisingly, the only scaffold with a dense cell growth on its bottom zone was the one of the dynamic culture.

After six days of culture we reevaluated cell distribution within the three representative zones of each studied scaffold (Fig. 8). Compared to 24 hours, the cells within the dynamic stirrer, apart from their great increase in their number, completely changed their distribution. Instead of gathering mainly on the bottom zone, they were now mostly found in the middle zone, keeping a rather even distribution. Cells on SW2S-on Air scaffolds preserved an even distribution within the zones, showing a slight affinity to the middle zone.

4. Discussion

After 24h, cells were viable in all scaffolds. The scaffolds with the most favorable performance were the static, wet scaffolds, seeded on both or only one side. The wet scaffolds on air (SW1S-on Air and SW2S-on Air) exhibited the least, non significant cell loss, making them the optimal scaffolds for static seeding. The wet scaffold on the dynamic stirrer on the other hand, exhibited a significant cell loss and was the least favorable scaffold for cell adhesion 24 hours after seeding.

Scaffolds seeded on both sides exhibited a better, more uniform distribution of cells within all zones at all timepoints. By the 6th day the majority of cells of the SW2S-on Air and of the dynamic stirrer scaffolds remained viable and exhibited an increase in their population, under both normoxia and hypoxia. The highest increase and highest number of cells was found on the dynamic scaffolds. The cells on SW2S-on Air scaffolds preserved their even distribution within the zones, showing a slight affinity to the middle zone.

4.1 Static technique with the newly developed device

In vitro static cultures are the most widely used in research and therefore have been intensively studied. Biotechnology companies and researchers around the world constantly try to overcome limitations or imperfections and to improve 3D culture methods and applications, creating new product designs. One of the drawbacks we detected in previous work is the attachment of cells, due to surface tension, on the surface of the well plate under the scaffold. Our effort in this study was to avoid the direct contact of the scaffolds with the well plate, which may lead to a relative cell loss, and to facilitate the circulation of fluids and nutrient supply within the scaffold by keeping both its surfaces free. We therefore created a static 3D-cell Culture Device (3D-CD) that can hold scaffolds on air and can easily be used with almost any kind of scaffold's

shape, with minimal adjustments. At 24 hours the scaffolds with the most favorable performance were the static, wet scaffolds on air (SW1S-on Air and SW2S-on Air) reaching 93.16% and 93.54% on cell seeding efficiency respectively, therefore making them the optimal scaffolds for static seeding.

Our on-Air scaffolds performed much better than the corresponding non-Air scaffolds used in the study. We tried to compare the efficiency of the on-Air scaffolds in our study with similar scaffolds used in other studies. It is of course impossible to make a complete and perfect comparison, because there are too many technical or experimental parameters used in each study, such as the scaffold material, or architecture, size etc., therefore there cannot be an absolute matching of the experimental conditions.

In a recent study with 3D printed, β -tricalcium phosphate (β -TCP), dry scaffolds, seeded on one side, only 21.75% of the MSCs remained attached (Fahimipour et al., 2019). This is less than the 28.51% of cells remaining in the corresponding SD1S-on Air scaffolds used in our study, where, overall, the dry scaffolds had the worst performance. In another study, top surface static seeding with 3T3-Swiss albino fibroblasts of prewetted PLGA scaffolds was the most favorable seeding technique (Thevenot et al., 2008). This resulted in approximately 62% cell efficiency, which is much lower than the 93.16% in our corresponding SW1S-on Air scaffold. A 3D scaffold made of polyactive foam was seeded on one side with chondrocytes (Wendt et al., 2003). In this study, cell seeding efficiency within the structure by cross sections reached 67%, very close to the efficiency in the corresponding SW1S scaffold used in our study, of 68.99%. Interestingly, as pointed before, the SW1S-on Air in our experiment reached 93.16%. It generally seems that the on-Air scaffolds perform better than other, similar, corresponding scaffolds.

At the 6th day, the cells on SW2S-on Air scaffolds preserved their even distribution within the zones, showing a slight affinity to the middle zone. This kind of colonization is optimal in a 3D culture, since the scaffold is intended to replace tissue deficiencies and high cell population, especially inside the scaffold, is highly appreciated. The on-Air scaffolds seem to exhibit a more favorable cell distribution when compared to corresponding, typical, statically seeded scaffolds in other studies, which usually appeared with more cells only on the surfaces of the scaffolds (Mauney et al., 2004).

4.2 Static-dynamic culture

Research studies comparing 3D static and dynamic cultures usually conclude that dynamic culture favors both cell adhesion and cell proliferation. There have been various approaches to dynamic cultures, with several methods of application, (Almarza & Athanasiou, 2004; Alvarez-Barreto & Sikavitsas, 2007; Bancroft et al., 2002; Freed et al., 1994; Freed et al., 1993; Leferink et al., 2016; Thevenot et al., 2008; Weinand et al., 2009; Wendt et al., 2003), with the spinner flask being the most commonly used technique.

PGA scaffolds, placed in well-mixed spinner flasks, were seeded with chondrocytes and aggregates and were observed after 24h. Cell seeding yield was essentially described to be 100% (G. Vunjak-Novakovic et al., 1998a). Polyactive foams were seeded with chondrocytes in the study of Wendt et al. (Wendt et al., 2003) and were cultured by two dynamic methods. The first was an oscillating perfusion technique with a U-cap bioreactor custom-made design and the second was a magnetically stirrer method based in Vunjak-Novakovic's technique (Gordana Vunjak-Novakovic et al., 1996; G. Vunjak-Novakovic et al., 1998a). When the cross sections of the scaffolds were analyzed, cell seeding efficiency in spinner flasks reached 77% and in the U-cap bioreactor reached 87%. In our study Vunjak-Novakovic's method was also applied, nevertheless, seeding efficiency at 24 hours was estimated to be much lower, 20,82%. In the study of Mauney J.R. et al. (Mauney et al., 2004), cubes of demineralized bone matrices (DMB) were seeded with almost the same technique as in our study. The dynamic seeding by spinner flask scaffolds resulted in approximately 3.6 times more cells (expressed in AU/mg by MTT cell absorbance units) compared to the prewetted static, double-side seeding scaffolds. In our study the results were reverse; there were 3.7 times more cells in the static double seeded, prewetted scaffolds than on the dynamic.

Considering that the dynamic method in our study was applied exactly as described in the original study by Vunjak-Novakovic G. et al. and Freed L.E. et al. (Freed et al., 1998; G. Vunjak-Novakovic et al., 1998b), we can only suggest that the difference in seeding efficiency is the result of different scaffold texture

and architecture. Nevertheless, after 6 days of proliferation in dynamic conditions in this study, the cell population exhibited more than a 20fold increase, which is surprisingly overall a better performance than in the previously described studies. Even though the initial population after 24 hours of seeding was much less than expected when having in mind similar experiments, proliferative rates in dynamic culture are obviously very high, even higher than expected. In the PGA scaffolds seeded within spinner flasks, cross section slices on day 1 revealed a 50 μm -thick surface zone with cell concentrations 60-70% higher than those in the bulk volume (G. Vunjak-Novakovic et al., 1998a). This is in agreement with our findings where zonal analysis revealed that the bottom zone of our scaffold exhibited a cell distribution of approximately 63.4%, much higher than the other zones. This may result from the mild centripetal force created during stirring, which generates a circular flow within the flask. We suggest that cells follow the flow towards the center of the rotating magnet and easily attach on the bottom side of the scaffold, facing the magnet.

Conclusions

The static 3D-cell Culture Device (3D-CD), which holds scaffolds on air, enhanced cell seeding efficiency and achieved almost no cell loss, fulfilling the requirements we set in our study design. A great advantage of the device is that it may be designed adapted to own needs and no extra equipment is required for its construction, since the same 3D printing technology for fabrication of scaffolds is used. In this study, the static culture conditions were optimized with the use of the device, which is very important considering that static culture is often preferred as a simpler method.

According to the results, the group of prewetted scaffolds was the most favorable to cell attachment independently of the cell seeding method used. Dynamic cell seeding did not reach our expectations and the effectiveness described by similar studies, probably due to the scaffolds we used and to parameters such as source of cells, scaffold's material and pore-interconnected architecture, were not favorable for this study design.

Nevertheless, despite the low number of cells at 24hours, after 6 days of proliferation the dynamic method resulted to a 20fold increase in the cell number, which is much higher than most of other dynamic seeding methods described. Therefore we suggest that, when handling this type of scaffolds and cells, the most favorable outcome will be produced with static double seeding in our 3D-cell Culture Device for 24 hours, followed by proliferation either in the same device or with dynamic culture as a hybrid technique.

References

- Almarza, A.J., & Athanasiou, K.A. (2004). Seeding techniques and scaffolding choice for tissue engineering of the temporomandibular joint disk. *Tissue Eng*, *10* (11-12), 1787-95. doi: 10.1089/ten.2004.10.1787
- Alvarez-Barreto, J.F., & Sikavitsas, V.I. (2007). Improved mesenchymal stem cell seeding on RGD-modified poly(L-lactic acid) scaffolds using flow perfusion. *Macromol Biosci*, *7* (5), 579-88. doi: 10.1002/mabi.200600280
- Bancroft, G.N., Sikavitsas, V.I., van den Dolder, J., Sheffield, T.L., Ambrose, C.G., Jansen, J.A., & Mikos, A.G. (2002). Fluid flow increases mineralized matrix deposition in 3D perfusion culture of marrow stromal osteoblasts in a dose-dependent manner. *Proc Natl Acad Sci U S A*, *99* (20), 12600-5. doi: 10.1073/pnas.202296599
- Bolte, S., & Cordelieres, F.P. (2006). A guided tour into subcellular colocalization analysis in light microscopy. *Journal of Microscopy-Oxford*, *224*, 213-32. doi: DOI 10.1111/j.1365-2818.2006.01706.x
- Choong, C.S., Hutmacher, D.W., & Triffitt, J.T. (2006). Co-culture of bone marrow fibroblasts and endothelial cells on modified polycaprolactone substrates for enhanced potentials in bone tissue engineering. *Tissue Eng*, *12* (9), 2521-31. doi: 10.1089/ten.2006.12.2521
- Correia, C., Bhumiratana, S., Yan, L.P., Oliveira, A.L., Gimble, J.M., Rockwood, D., Kaplan, D.L., Sousa, R.A., Reis, R.L., & Vunjak-Novakovic, G. (2012). Development of silk-based scaffolds for tis-

sue engineering of bone from human adipose-derived stem cells. *Acta Biomater*, 8 (7), 2483-92. doi: 10.1016/j.actbio.2012.03.019

Dawson, E., Mapili, G., Erickson, K., Taqvi, S., & Roy, K. (2008). Biomaterials for stem cell differentiation. *Adv Drug Deliv Rev*, 60 (2), 215-28. doi: 10.1016/j.addr.2007.08.037

Fahimipour, F., Dashtimoghadam, E., Mahdi Hasani-Sadrabadi, M., Vargas, J., Vashae, D., Lobner, D.C., Jafarzadeh Kashi, T.S., Ghasemzadeh, B., & Tayebi, L. (2019). Enhancing cell seeding and osteogenesis of MSCs on 3D printed scaffolds through injectable BMP2 immobilized ECM-Mimetic gel. *Dent Mater*, 35 (7), 990-1006. doi: 10.1016/j.dental.2019.04.004

Freed, L.E., Hollander, A.P., Martin, I., Barry, J.R., Langer, R., & Vunjak-Novakovic, G. (1998). Chondrogenesis in a cell-polymer-bioreactor system. *Experimental Cell Research*, 240 (1), 58-65. doi: DOI 10.1006/excr.1998.4010

Freed, L.E., Marquis, J.C., Langer, R., Vunjak-Novakovic, G., & Emmanuel, J. (1994). Composition of cell-polymer cartilage implants. *Biotechnol Bioeng*, 43 (7), 605-14. doi: 10.1002/bit.260430710

Freed, L.E., Vunjak-Novakovic, G., & Langer, R. (1993). Cultivation of cell-polymer cartilage implants in bioreactors. *J Cell Biochem*, 51 (3), 257-64. doi: 10.1002/jcb.240510304

Hofmann, S., Knecht, S., Langer, R., Kaplan, D.L., Vunjak-Novakovic, G., Merkle, H.P., & Meinel, L. (2006). Cartilage-like tissue engineering using silk scaffolds and mesenchymal stem cells. *Tissue Engineering*, 12 (10), 2729-38. doi: DOI 10.1089/ten.2006.12.2729

Karageorgiou, V., & Kaplan, D. (2005). Porosity of 3D biomaterial scaffolds and osteogenesis. *Biomaterials*, 26 (27), 5474-91. doi: 10.1016/j.biomaterials.2005.02.002

Kim, B.S., Putnam, A.J., Kulik, T.J., & Mooney, D.J. (1998). Optimizing seeding and culture methods to engineer smooth muscle tissue on biodegradable polymer matrices. *Biotechnology and Bioengineering*, 57 (1), 46-54.

Langer, R., & Vacanti, J.P. (1993). Tissue engineering. *Science*, 260 (5110), 920-6. doi: 10.1126/science.8493529

Lavrentieva, A., Majore, I., Kasper, C., & Hass, R. (2010). Effects of hypoxic culture conditions on umbilical cord-derived human mesenchymal stem cells. *Cell Commun Signal*, 8 , 18. doi: 10.1186/1478-811X-8-18

Leferink, A.M., Hendrikson, W.J., Rouwkema, J., Karperien, M., van Blitterswijk, C.A., & Moroni, L. (2016). Increased cell seeding efficiency in bioplotting three-dimensional PEOT/PBT scaffolds. *J Tissue Eng Regen Med*, 10 (8), 679-89. doi: 10.1002/term.1842

Loh, Q.L., & Choong, C. (2013). Three-dimensional scaffolds for tissue engineering applications: role of porosity and pore size. *Tissue Eng Part B Rev*, 19 (6), 485-502. doi: 10.1089/ten.TEB.2012.0437

Luo, F., Hou, T.Y., Zhang, Z.H., Xie, Z., Wu, X.H., & Xu, J.Z. (2013). Effects of Initial Cell Density and Hydrodynamic Culture on Osteogenic Activity of Tissue-Engineered Bone Grafts. *Plos One*, 8 (1). doi: ARTN e53697 10.1371/journal.pone.0053697

Martinez-Ramos, C., Valles-Lluch, A., Verdugo, J.M., Ribelles, J.L., Barcia Albacar, J.A., Orts, A.B., Soria Lopez, J.M., & Pradas, M.M. (2012). Channeled scaffolds implanted in adult rat brain. *J Biomed Mater Res A*, 100 (12), 3276-86. doi: 10.1002/jbm.a.34273

Mauney, J.R., Blumberg, J., Pirun, M., Volloch, V., Vunjak-Novakovic, G., & Kaplan, D.L. (2004). Osteogenic differentiation of human bone marrow stromal cells on partially demineralized bone scaffolds in vitro. *Tissue Eng*, 10 (1-2), 81-92. doi: 10.1089/107632704322791727

Merceron, C., Vinatier, C., Portron, S., Masson, M., Amiaud, J., Guigand, L., Cherel, Y., Weiss, P., & Guicheux, J. (2010). Differential effects of hypoxia on osteochondrogenic potential of human adipose-derived

stem cells. *Am J Physiol Cell Physiol*, 298 (2), C355-64. doi: 10.1152/ajpcell.00398.2009

Nair, L.S., & Laurencin, C.T. (2007). Biodegradable polymers as biomaterials. *Progress in Polymer Science*, 32 (8), 762-98. doi: <https://doi.org/10.1016/j.progpolymsci.2007.05.017>

Rodina, A.V., Tenchurin, T.K., Saprykin, V.P., Shepelev, A.D., Mamagulashvili, V.G., Grigor'ev, T.E., Lukanina, K.I., Orekhov, A.S., Moskaleva, E.Y., & Chvalun, S.N. (2016). Migration and Proliferative Activity of Mesenchymal Stem Cells in 3D Polylactide Scaffolds Depends on Cell Seeding Technique and Collagen Modification. *Bull Exp Biol Med*, 162 (1), 120-26. doi: 10.1007/s10517-016-3560-6

Sheehy, E.J., Buckley, C.T., & Kelly, D.J. (2012). Oxygen tension regulates the osteogenic, chondrogenic and endochondral phenotype of bone marrow derived mesenchymal stem cells. *Biochem Biophys Res Commun*, 417 (1), 305-10. doi: 10.1016/j.bbrc.2011.11.105

Theodoridis, K., Aggelidou, E., Manthou, M., Demiri, E., Bakopoulou, A., & Kritis, A. (2019). Assessment of cartilage regeneration on 3D collagen-polycaprolactone scaffolds: Evaluation of growth media in static and in perfusion bioreactor dynamic culture. *Colloids Surf B Biointerfaces*, 183, 110403. doi: 10.1016/j.colsurfb.2019.110403

Theodoridis, K., Aggelidou, E., Vavilis, T., Manthou, M.E., Tsimponis, A., Demiri, E.C., Boukla, A., Salpistis, C., Bakopoulou, A., Mihailidis, A., & Kritis, A. (2019). Hyaline cartilage next generation implants from adipose-tissue-derived mesenchymal stem cells: Comparative study on 3D-printed polycaprolactone scaffold patterns. *J Tissue Eng Regen Med*, 13 (2), 342-55. doi: 10.1002/term.2798

Thevenot, P., Nair, A., Dey, J., Yang, J., & Tang, L. (2008). Method to analyze three-dimensional cell distribution and infiltration in degradable scaffolds. *Tissue Eng Part C Methods*, 14 (4), 319-31. doi: 10.1089/ten.tec.2008.0221

Vunjak-Novakovic, G., Freed, L.E., Biron, R.J., & Langer, R. (1996). Effects of mixing on the composition and morphology of tissue-engineered cartilage. *AIChE Journal*, 42 (3), 850-60. doi: 10.1002/aic.690420323

Vunjak-Novakovic, G., Obradovic, B., Martin, I., Bursac, P.M., Langer, R., & Freed, L.E. (1998a). Dynamic cell seeding of polymer scaffolds for cartilage tissue engineering. *Biotechnol Prog*, 14 (2), 193-202. doi: 10.1021/bp970120j

Vunjak-Novakovic, G., Obradovic, B., Martin, I., Bursac, P.M., Langer, R., & Freed, L.E. (1998b). Dynamic cell seeding of polymer scaffolds for cartilage tissue engineering. *Biotechnology Progress*, 14 (2), 193-202. doi: 10.1021/Bp970120j

Weinand, C., Xu, J.W., Peretti, G.M., Bonassar, L.J., & Gill, T.J. (2009). Conditions affecting cell seeding onto three-dimensional scaffolds for cellular-based biodegradable implants. *J Biomed Mater Res B Appl Biomater*, 91 (1), 80-7. doi: 10.1002/jbm.b.31376

Wendt, D., Marsano, A., Jakob, M., Heberer, M., & Martin, I. (2003). Oscillating perfusion of cell suspensions through three-dimensional scaffolds enhances cell seeding efficiency and uniformity. *Biotechnology and Bioengineering*, 84 (2), 205-14. doi: 10.1002/bit.10759

| 3D Scaffold design characteristics |
|------------------------------------|------------------------------------|------------------------------------|------------------------------------|------------------------------------|------------------------------------|------------------------------------|
| Scaffold design pattern | Φβερ
διαμετερ μμ | Λαψερ
ηειγητ μμ | Infill density
% | Pore shapes
geometry | Scaffold porosity % | Scaffold porosity with Image J % |

3D Scaffold design characteristics	3D Scaffold design characteristics	3D Scaffold design characteristics				
Honeycomb	400	300	55	Rectangular & Hexagonal 150~700 [?] 425	83.4 ± 0.43	82.9 ± 0.37

Table 1: Scaffold fabrication and geometrical characteristics, pore sizes and scaffold porosity

Figure legends

Figure 1:

Design of the static 3D-cell Culture Device (3D-CD) (A), cell seeding on both sides by easily twisting the device with the scaffold (B), nutrient supply (C).

Figure 2:

Static seeding for both wet and dry groups illustrating as SW1S / SD1S (I.A), SW2S / SD2S (I.B), SW1S-on Air / SD1S-on Air (I.C), SW2S-on Air / SD2S-on Air (I.D). Dynamic seeding in magnetic stirrer flask (II)

Figure 3:

Plot of a polygon region (R1) created from side-scattered light (SSC) and forward-scattered light (FSC). The polygon region separates cells from debris.

Figure 4:

Cell viability with confocal microscopy on both surfaces and cross sections of the scaffolds under static culture parameters (A), and in dynamic culture under normoxia and hypoxia culture conditions (B). Images are merged for live and dead cells

Figure 5:

Cell seeding efficiency after 24 hours, for both static and dynamic seeding techniques (A). Cell proliferation on the best performance of static method and dynamic method cultured for 6days (B). Cells measured as absolute cell numbers within Guava easyCyte flow cytometer.

Figure 6:

Micro-CT scans and 3D volume renderings. 3D rendered images of the scanned specimens were created to visually represent cell distribution and orientation after 24h and after 6 days of the cells inside the scaffolds

Figure 7:

Three representative zones (top, middle and bottom) created from 2D slices of m-CT stacks for cell attachment after 24h. 3D surface of cell attachment expressed in percentage %, was analyzed with Image J 3D Object Counter plug in (A), and histogram-like visualization of cell arrangement within the 3 zones of the scaffold after cell seeding has been plotted with the 3D surface plot tool from image J (B)

Figure 8:

Three representative zones (top, middle and bottom) created from 2D slices of m-CT stacks for cell proliferation after 6 days. 3D surface of cell attachment expressed in percentage %, was analyzed with Image J 3D

Object Counter plug in (A), and histogram-like visualization of cell arrangement within the 3 zones of the scaffold after cell seeding has been plotted with the 3D surface plot tool from image J (B)

Ethics approval and consent to participate

The study has been approved by the Ethics Committee, of the Institutional Review Board of the School of Medicine, Faculty of Health Sciences, Aristotle University of Thessaloniki reference number 555/1-10-2015 and tissue donation was under Papageorgiou Hospital Review Board approved protocols 263-7/12/2016 signed informed consent according to the Helsinki Protocol.

Competing interests

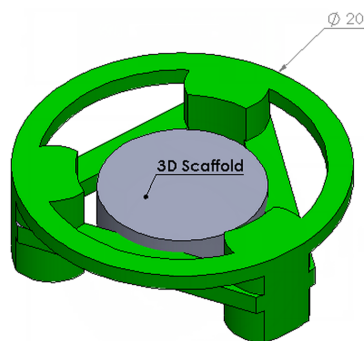
The authors declare that they have no competing interests.

Data Availability Statement

The datasets supporting the results of this article are included within the article

Author contributions: AK conceived and coordinated the study, supervised experiments, analyzed and interpreted the data and drafted the manuscript. EA performed the cell culture and molecular analysis of the samples. KT conceived and fabricated the 3D-cell Culture Device (3D-CD), designed the produced 3D printed scaffolds, performed the experiments participated in cell culturing, analyzed and interpreted data and contributed to drafting of the manuscript. MM participated methodology establishment, supervised the confocal analysis analyzed and interpreted data and critically reviewed the manuscript. KK performed the micro-Computed Tomography and analyzed the data. ED and TA participated in the study design, provided adipose tissue samples and contributed to drafting of the manuscript. BA supervised the confocal analysis and critically reviewed the manuscript. MA supervised experiments, helped for the construction of the 3D-cell Culture Device (3D-CD) and critically reviewed the manuscript. All authors read and approved the final manuscript.

A. Device design (3D-CD)



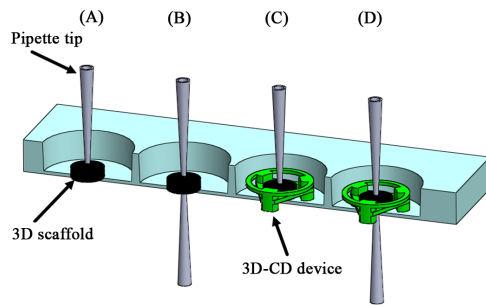
B. Cell seeding on both sides



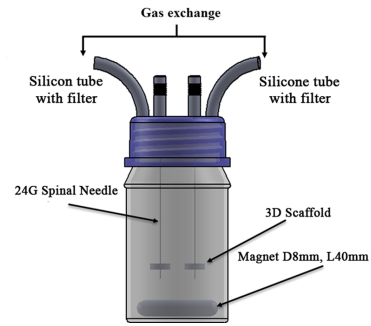
C. Nutrient supply



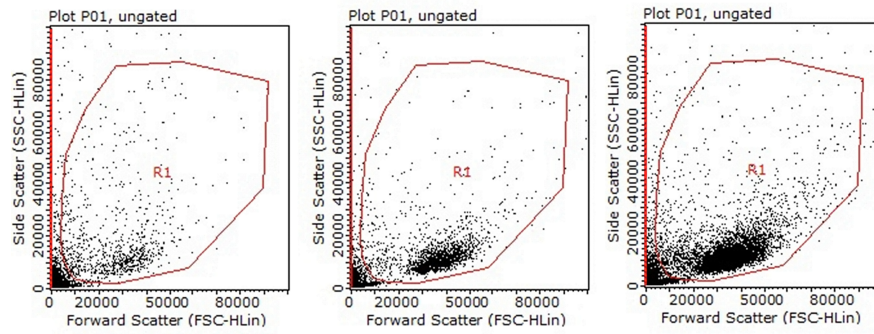
I. Static cell seeding

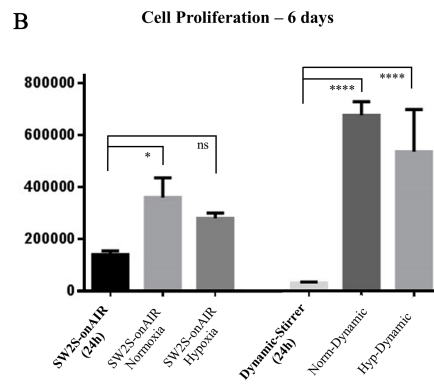
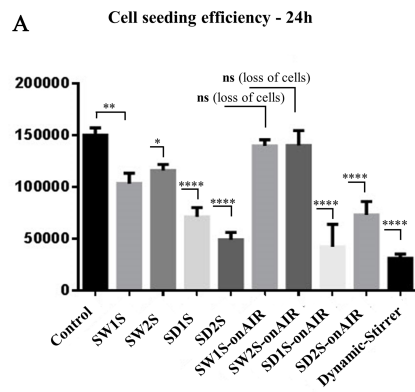
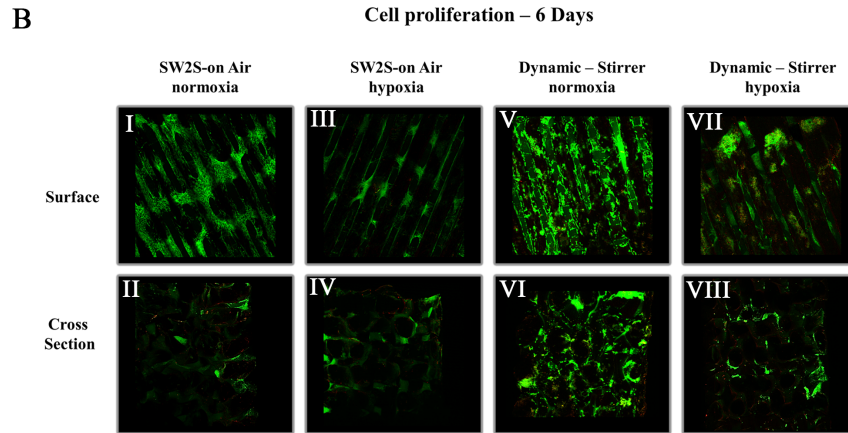
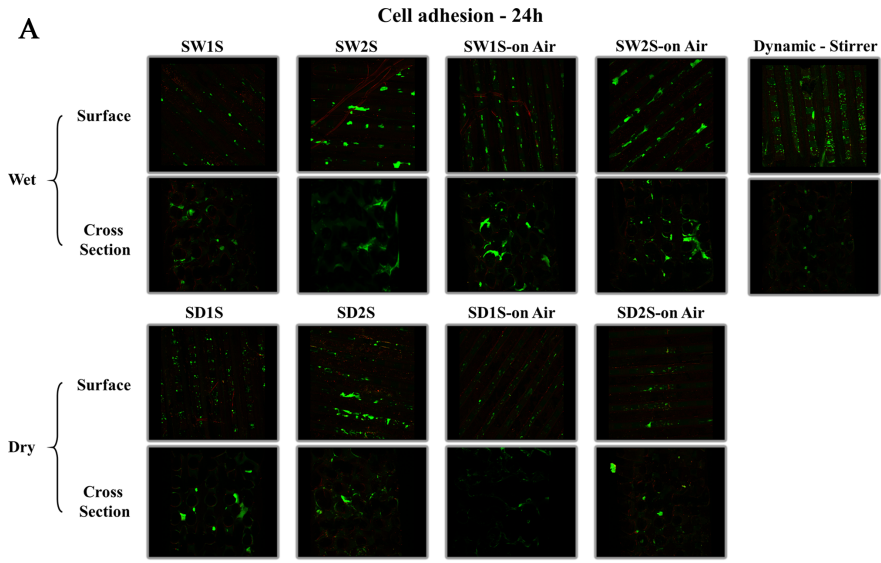


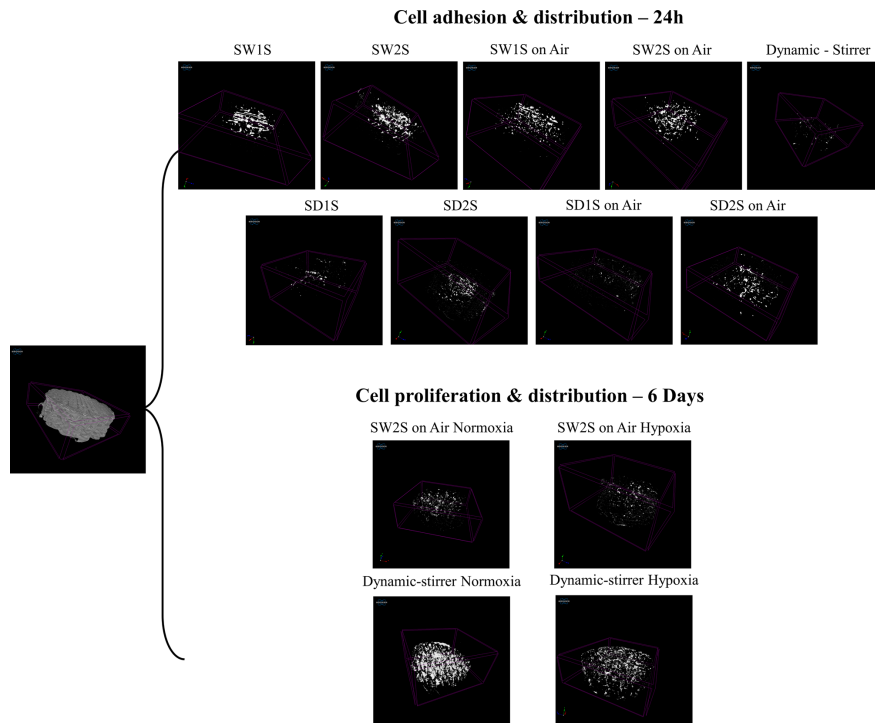
II. Dynamic cell seeding



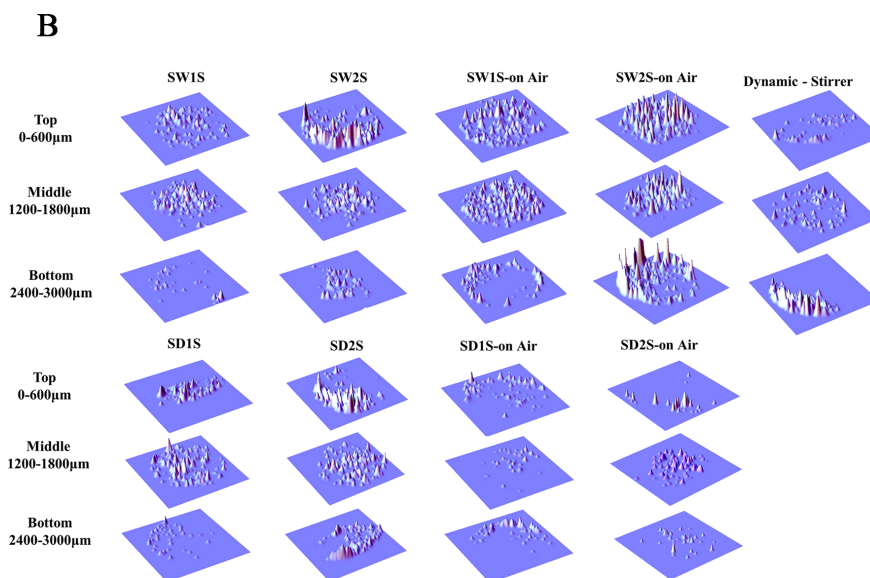
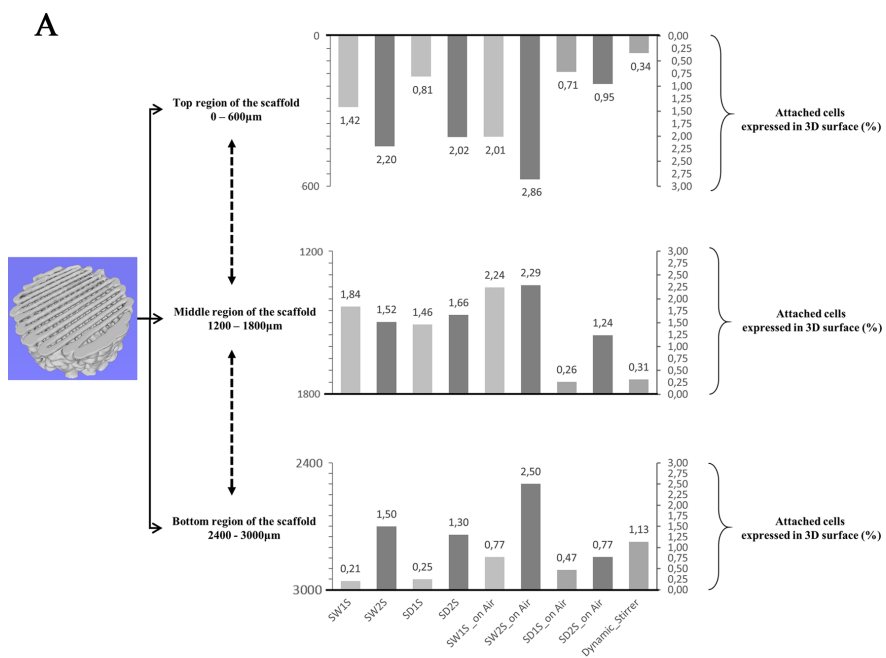
Absolute cell counting







Cell adhesion and distribution within zones - 24h



Cell proliferation and distribution within zones - 6 Days

